

Graft-versus-host disease disrupts intestinal microbial ecology by inhibiting Paneth cell production of α -defensins

Yoshihiro Eriguchi,¹ Shuichiro Takashima,¹ Hideyo Oka,¹ Sonoko Shimoji,¹ Kiminori Nakamura,² Hidetaka Uryu,¹ Shinji Shimoda,¹ Hiromi Iwasaki,³ Nobuyuki Shimono,¹ Tokiyoshi Ayabe,² Koichi Akashi,^{1,3} and Takanori Teshima³

¹Department of Medicine and Biosystemic Science, Kyushu University Graduate School of Medical Science, Fukuoka, Japan; ²Department of Cell Biological Science, Graduate School of Life Science, Faculty of Advanced Life Science, Hokkaido University, Sapporo, Japan; and ³Center for Cellular and Molecular Medicine, Kyushu University Graduate School of Medical Science, Fukuoka, Japan

Allogeneic hematopoietic stem cell transplantation (SCT) is a curative therapy for various hematologic disorders. Graft-versus-host disease (GVHD) and infections are the major complications of SCT, and their close relationship has been suggested. In this study, we evaluated a link between 2 complications in mouse models. The intestinal microbial communities are actively regulated by Paneth cells through their secretion of antimicrobial peptides, α -defensins. We discovered that Paneth cells are targeted by

GVHD, resulting in marked reduction in the expression of α -defensins, which selectively kill noncommensals, while preserving commensals. Molecular profiling of intestinal microbial communities showed loss of physiologic diversity among the microflora and the overwhelming expansion of otherwise rare bacteria *Escherichia coli*, which caused septicemia. These changes occurred only in mice with GVHD, independently on conditioning-induced intestinal injury, and there was a significant correlation between alteration

in the intestinal microbiota and GVHD severity. Oral administration of polymyxin B inhibited outgrowth of *E coli* and ameliorated GVHD. These results reveal the novel mechanism responsible for shift in the gut flora from commensals toward the widespread prevalence of pathogens and the previously unrecognized association between GVHD and infection after allogeneic SCT. (*Blood*. 2012;120(1): 223-231)

Introduction

Allogeneic hematopoietic stem cell transplantation (SCT) is a curative therapy for hematologic malignant tumors, bone marrow failure, and congenital metabolic disorders. Graft-versus-host disease (GVHD) and related infections are major obstacles to SCT, and their close relationship has been indicated in clinical settings. Septicemia is the most life-threatening infection after allogeneic SCT and gram-negative rods are the most dominant pathogens of septicemia, whereas incidence of drug-resistant enterococci infection increase in neutropenic patients colonized with these bacteria in some centers.¹ GVHD is one of the major predisposing factors for the development of septicemia.² Since the pioneering works of van Bekkum³ and others in the 1960s-1970s, interaction between intestinal flora and GVHD has been suggested.³⁻⁶

We recently demonstrated that intestinal stem cells (ISCs), which are essential to repair damaged intestinal epithelium, are targeted by GVHD.⁷ Recently, Paneth cells located besides ISCs within the crypts are identified as niche for ISCs.⁸ In addition, Paneth cells are essential regulators of the composition of intestinal microbiota by secreting antimicrobial peptides, α -defensins, which provide broad-spectrum antimicrobial properties by pore formation in the bacterial cell walls.⁹⁻¹¹ The intestine, which is the major interface between the environment and the host, is an open ecologic system that is colonized by at least 1000 distinct bacterial species, of which more than 80% are nonculturable.¹²⁻¹⁴ Accurate identification of species in the gut microbiota requires culture-independent, molecular profiling methods. Firmicutes and Bacteroidetes make

up approximately 90% of the intestinal microbiota.^{12,15} These commensals are rarely pathogenic and instead make several essential contributions to human physiology and health.^{12,13,15,16} In contrast, Gammaproteobacteria such as *Escherichia coli*, which have a gram-negative cell wall make up a small proportion of the microbiota.¹⁷ A recent study showed an increase in gram-negative *Enterobacteriaceae* family members including *E coli* among the intestinal microbiota after allogeneic bone marrow transplantation (BMT) in mice.¹⁸ It remains unclear why they are most frequent pathogens in patients with intestinal GVHD, although the role of systemic immunosuppression and use of antibiotics has been well appreciated.¹⁹

In this study, we focused on Paneth cells and evaluated the possible mechanistic links between GVHD and infection in mouse models of BMT. We found that GVHD targets Paneth cells and causes subsequent impairment of antimicrobial peptide secretion, leading to marked loss of diversity among the intestinal microflora. This results in shift in the gut flora from commensal microorganisms toward the widespread prevalence of gram-negative bacteria and development of bloodstream infection.

Methods

Mice

Female C57BL/6 (B6: H-2^b), B6D2F1 (H-2^{b/d}), B6C3F1 (H-2^{b/k}), B6-Ly5.1 (H-2^b, CD45.1⁺), and C3H.Sw (H-2^b) mice were purchased from Charles

Submitted December 25, 2011; accepted April 22, 2012. Prepublished online as *Blood* First Edition paper, April 24, 2012; DOI 10.1182/blood-2011-12-401166.

There is an Inside *Blood* commentary on this article in this issue.

The publication costs of this article were defrayed in part by page charge payment. Therefore, and solely to indicate this fact, this article is hereby marked "advertisement" in accordance with 18 USC section 1734.

© 2012 by The American Society of Hematology

River Japan, KBT Oriental, or Japan SLC. All animal experiments were performed under the auspices of the Institutional Animal Care and Research Advisory Committee.

BMT

Mice were transplanted as previously described.²⁰ In brief, after lethal x-ray total body irradiation (TBI) delivered in 2 doses at 4-hour intervals, mice were intravenously injected with 5×10^6 T-cell depleted bone marrow (TCD-BM) cells with or without 2×10^6 splenic T cells on day 0. Isolation of T cells and T-cell depletion were performed using the T-cell isolation kit and anti-CD90 microBeads, respectively, and the AutoMACS (Miltenyi Biotec) according to the manufacturer's instructions. In some experiments, unirradiated B6D2F1 mice were intravenously injected with 12×10^7 splenocytes.⁷ Mice were maintained in specific pathogen-free conditions and received normal chow and autoclaved hyperchlorinated water (Ph 4) for the first 3 weeks after BMT and filtered water thereafter. Polymyxin B (Calbiochem) diluted in water was administered by daily oral gavage at a dose of 100 mg/kg from day -4 until day 28 after BMT. Survival after BMT was monitored daily and the degree of clinical GVHD was assessed weekly by a scoring system which sums changes in 5 clinical parameters: weight loss, posture, activity, fur texture, and skin integrity (maximum index = 10) as previously described.²⁰

Histologic and immunohistochemical analysis

For pathologic analysis, samples of the small intestine were fixed in 10% neutral-buffered formalin, embedded in paraffin, sectioned, slide mounted, and stained with H&E. Immunohistochemistry was performed as described²¹ using rabbit anti-lysozyme (Dako) and rabbit anti-defensin1. Histofine simple stain MAX PO (Rat) kits and subsequently diaminobenzide (DAB) solution (Nichirei Biosciences) was used to generate brown-colored signals. Slides were then counterstained with hematoxylin. Pictures from tissue sections were taken at room temperature using a digital camera (DP72; Olympus) mounted on a microscope (BX51; Olympus). Acute GVHD was assessed by detailed histopathologic analysis using a semiquantitative scoring system.²²

Preparation and analysis of isolated mouse crypts

Individual crypts were isolated from the small intestine as previously described.²³ Isolated crypts were fixed with 2% paraformaldehyde in PBS for 20 minutes and permeabilized with 0.2% Triton X-100 in PBS for 5 minutes. Crypts were incubated for 1 hour with fluorescein isothiocyanate-conjugated anti-lysozyme (10 μ g/mL; Dako), washed 3 times in PBS, followed by incubation for 1 hour with Alexa Fluor 594-conjugated phalloidin (1 U/mL; Invitrogen). Tetramethyl 4,6-diamidino-2-phenylindole (DAPI; 5 μ g/mL; Invitrogen) was used to stain the nucleus. Samples were mounted in aqua poly/mount (Polysciences) and examined with a confocal laser-scanning microscope (LSM510; Carl Zeiss).

Enzyme-linked immunosorbent assay

The limulus amebocyte lysate assay QCL-1000 (Lonza) was performed according to the manufacturer's instructions to determine the serum level of lipopolysaccharide (LPS) with a sensitivity of 0.1 EU/mL. All units expressed are relative to the United States reference standard EC-2.

Quantitative real-time PCR analysis

Total RNA was purified using the RNeasy Kit (QIAGEN). cDNA was synthesized using a QuantiTect reverse transcription kit (QIAGEN). Polymerase chain reactions (PCRs) and analyses were performed with ABI PRISM 7900HT SDS 2.1 (Applied Biosystems) using TaqMan universal PCR master mix (Applied Biosystems), and TaqMan gene expression assays (Defa1: Mm02524428_g1, Defa4: Mm00651736_g1, Defa5: Mm00651548_g1, Defa21/Defa22: Mm04206099_gH, Defcr-rs1: Mm00655850_m1, Lyz1: Mm00657323_m1, and Gapdh: Mm9999915_g1; Applied Biosystems). The relative amount of each mRNA was determined using the standard curve method and was normalized to the level of GAPDH in each sample.

Total fecal bacterial DNA extraction

Total DNA was isolated from fecal pellets using a QIAamp DNA stool mini kit (QIAGEN) with bead beating treatment during the cell-lysis step. Briefly, fresh fecal pellets were collected from individual mice; 0.5 g baked 0.1 mm zirconia/silica beads (Biospec Products) and ASL buffer were added to each aliquot. Fecal samples with ASL buffer were incubated at 95°C, and samples were processed for 1 minute at speed 5.5 on Fastprep system (Qbiogene).²⁴

PCR amplification of 16S rRNA gene

Bacterial 16S ribosomal RNA (rRNA) genes were amplified with bacterial-universal primers, 27F (5'-AGAGTTTGATCTGGCTCAG-3') labeled at the 5' end with 6-carboxyfluorescein (6-FAM) and 1492R (5'-GGTTACCTTGT TACGACTT-3').²⁵ PCR amplification was performed using *EX Taq* (Takara Bio) and the following program: 3 minutes of denaturation at 95°C, 30 cycles of 0.5 minute at 95°C, 0.5 minute at 50°C, 1.5 minute at 72°C, and a final 10 minutes extension step at 72°C in a BiometraT3 thermocycler (Biometra). Amplicons were purified using a QIAquick PCR Purification kit (QIAGEN).

Restriction fragment length polymorphism (RFLP) analysis

The purified DNA products (3 μ L) were digested with 10 U of either *HhaI* or *MspI* (Takara Bio) in a total volume of 10 μ L at 37°C for 3 hours. The restriction digest products (2 μ L) were mixed with 10 μ L deionized formamide and 0.5 μ L GeneScan-1200 LIZ standard (Applied Biosystems). The samples were denatured at 95°C for 2 minutes, followed by rapid chilling on ice. The fluorescently labeled fragments (T-RFs) were separated by size on an ABI 3130 genetic analyzer (Applied Biosystems). The electropherograms were analyzed with GeneMapper Version 4.0 software (Applied Biosystems), and the fragment sizes were estimated using the Local Southern method. Each unique RFLP pattern was designated as an operational taxonomic unit (OTU). OTUs with a peak area of less than 0.5% of the total area were excluded from the analysis. Proportion of *E coli* was defined as the ratio of area of OTU for *E coli* to total areas of OTUs. Diversity of the microbial community corresponding to the RFLP banding pattern was calculated using the Simpson index of diversity 1-D ($D = \sum pi^2$)²⁶ and Shannon diversity index H' ($H' = -\sum pi \ln(pi)$)²⁷ and where pi is the proportion of total number of species made up of its species.

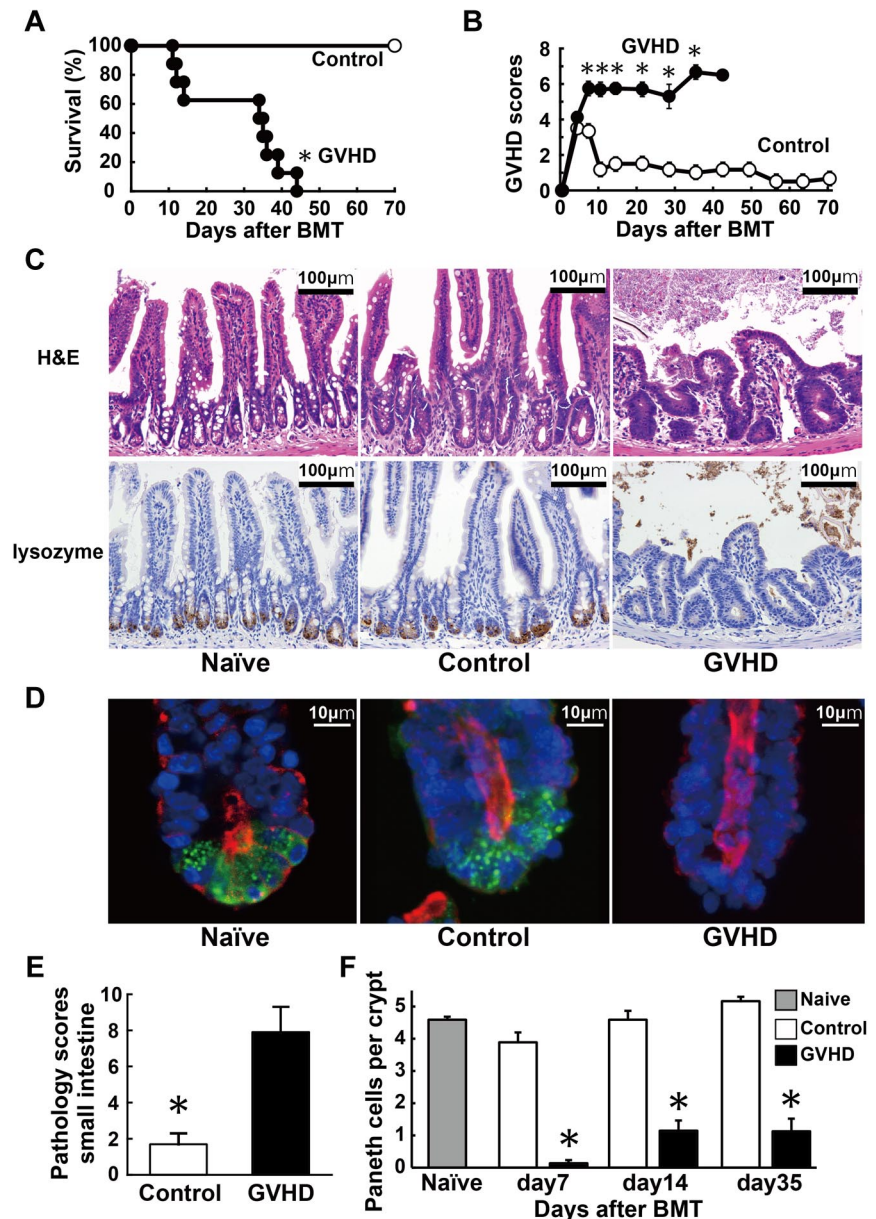
Cloning and sequencing analysis

Internal region of the 16S rRNA genes were amplified using 27F and 806R (5'-GGACTACCAGGGTATCTAAT-3') primers, and were transformed using TOPO TA Cloning Kit with TOP10 *E coli* (Invitrogen). The nucleotide sequences of inserts were determined using the M13 forward and reverse primers. All sequences were examined for possible chimeric artifacts by the Chimera check with Bellerophon Version 3. After eliminating chimeric sequences, the partial 16S rRNA sequences were compared with the sequences in the Ribosomal Database Project and GenBank, using the BLAST program (<http://www.ncbi.nlm.nih.gov/BLAST/>). Cloned sequences were identified as representing the species or phylotype of the sequence with the highest matching score. Sequences with less than 98% identity with a GenBank sequence were defined as a new phylotype. In addition, we checked whether the sequenced clones had the correct T-RFs compared with the sequence information.

Microbiologic analysis of bacterial translocation

The livers and mesenteric lymph nodes (mLNs) isolated from mice that had received transplants were removed aseptically and homogenized in 1 mL saline. Then, 500 μ L of homogenate was transferred into a tube containing 4.5 mL of saline and used to perform 4 serial dilutions. From this dilution, 100 μ L aliquots were cultured aerobically on blood agar and LB agar plates (Difco) for 24 hours at 37°C in room air supplemented with 10% CO₂. Colony-forming units (CFUs) were counted and adjusted per organ. Bacteria were identified by biochemical profiles.

Figure 1. Paneth cell injury in GVHD. Lethally irradiated B6D2F1 mice were transplanted with 5×10^6 TCD BM cells without (control group, $n = 6$) or with 2×10^6 T cells (GVHD group, $n = 12$) from MHC-mismatched B6 donors on day 0. (A-B) Survival (A) and clinical GVHD scores (B) means \pm SE are shown. Data from 2 independent experiments were combined. (C-F) Small intestines were isolated from mice 7 days after BMT. (C) Top panels: histology of the small intestine stained with H&E. Bottom panels: Lysozyme staining (brown). Magnification: $100\times$. Bars, $100 \mu\text{m}$. (D) Confocal cross-sectioning of the isolated small intestinal crypt. Lysozyme (green) is expressed by Paneth cells. Tetramethyl DAPI (blue) stains the nucleus and phalloidin (red) stains F-actin. Magnification: $1000\times$. Bars, $10 \mu\text{m}$. (E) Pathology scores of the small intestine (mean \pm SE, $n = 3-6$ / group). (F) Quantification of Paneth cells per crypt (mean \pm SE, $n = 3-6$ / group; $*P < .05$).



Statistical analysis

Mann-Whitney *U* tests were used to compare data, the Kaplan-Meier product limit method was used to obtain survival probability, and the log-rank test was applied to compare survival curves. To determine the statistically significant correlation, the Spearman rank correlation coefficient (*R*) was adopted. All tests were performed with SigmaPlot Version 10.0 software. $P < .05$ was considered statistically significant.

Accession numbers

Sequence data are available in the GenBank (<http://www.ncbi.nih.gov/genbank>) under the accession number 1509996.

Results

Paneth cell damage and decreased expression of α -defensins in GVHD

We evaluated whether Paneth cells could be damaged during GVHD. Lethally irradiated B6D2F1 (H-2^{bd}) mice received 5×10^6 TCD-BM

cells (control group) or these cells plus 2×10^6 T cells (GVHD group) from major histocompatibility complex (MHC)-mismatched B6 (H-2^b) donors on day 0. The allogeneic animals developed severe GVHD and all of these mice died within 50 days after BMT, whereas all TCD-BM controls survived through this period (Figure 1A). The surviving allogeneic animals showed significantly more severe signs of GVHD than controls, as assessed by clinical GVHD scores²⁰ (Figure 1B). Pathologic analysis of the small intestine 7 days after BMT showed mostly normal architecture in controls, whereas severe blunting of villi and inflammatory infiltration were observed in the GVHD group (Figure 1C). Paneth cells, which are typically identified microscopically by their location in the crypts and by the large granules occupying most of their cytoplasm, were hardly observed in the GVHD group. Immunohistochemical analysis for lysozyme, which indicates the presence of Paneth cells, confirmed loss of Paneth cells in the GVHD group, but not in controls (Figure 1C). Confocal cross-sectioning of individual crypts isolated from the small intestine further confirmed Paneth cell loss in these mice (Figure 1D). In mice with GVHD, GVHD pathology scores were significantly higher (Figure 1E), whereas numbers of Paneth cells

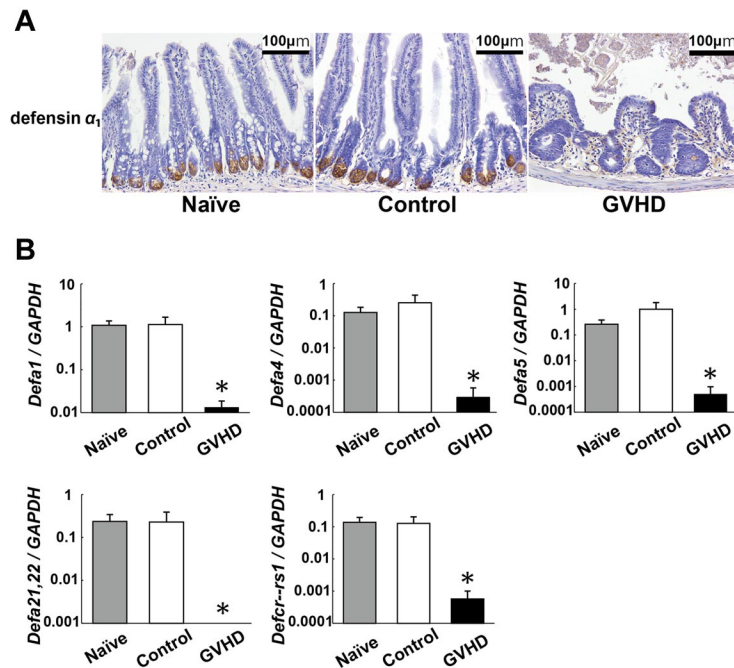


Figure 2. Decreased expression of Paneth cell–derived α -defensins in GVHD. Lethally irradiated B6D2F1 mice were transplanted with 5×10^6 TCD BM without (control group) or with (GVHD group) 2×10^6 T cells from B6 donors. Small intestines were isolated from mice 7 days after BMT. (A) Immunohistochemical staining for defensin α_1 (brown). Magnification: 100 \times . Bars, 100 μ m. (B) RNA was extracted from samples and quantitative real-time PCR analysis for enteric defensins including *Defa1*, *Defa4*, *Defa5*, *Defa21,22*, and *Defcr-rs1* was performed ($n = 6$ / group). Data are representative of 2 similar experiments and are shown as mean \pm SE ($*P < .05$).

were significantly and constantly lower compared with those in controls after BMT (Figure 1F).

α -Defensins are the major antimicrobial peptides produced by Paneth cells.²³ We evaluated the expression levels of enteric defensin families in the small intestines. Defensin α_1 expression was limited in Paneth cells in the crypts of naive mice (Figure 2A). Expression of defensin α_1 was preserved in controls 7 days after BMT but was severely suppressed in mice with GVHD. Quantitative real-time PCR analysis of the terminal ileum confirmed the reduced expression of *defensin- α_1* (*Defa1*) and other enteric defensin family members, including *Defa5*, *Defa21,22*, and *defensin α -related sequence 1* (*Defa-rs1*) in the small intestine of GVHD mice (Figure 2B). These results demonstrate that GVHD targets Paneth cells and limits the expression of Paneth cell–derived defensin family members.

Perturbation of normal intestinal microbiota in GVHD

Paneth cell–derived α -defensins are essential regulators of the microbiota composition in the intestine.¹¹ α -defensins have selective bactericidal activity against noncommensals, whereas exhibiting minimal bactericidal activity against commensals.^{28,29} We therefore hypothesized that the reduced expression of α -defensins results in dysbiosis in the intestinal microbial community. To test this hypothesis, we evaluated changes in the gut flora during the course of GVHD in a B6 \rightarrow B6D2F1 murine model of BMT without administering any antibiotic or immunosuppressive drugs. Before and after BMT, fecal pellets were collected from each mouse once per week. The composition of the intestinal microflora was determined by RFLP analysis of bacteria-specific 16S rRNA genes that were constructed from each sample of fecal pellets.^{30,31} Representative RFLP analysis is shown in Figure 3A. Each unique RFLP pattern is designated by an OTU that corresponds to specific species of bacteria. The peak height of each OTU indicates its relative quantity among the intestinal microflora and the number of OTUs indicates the diversity of flora. Before BMT, multiple OTUs were observed with little interindividual variation among the RFLP patterns (Figure 3A left panels). Seven days after BMT, numbers of

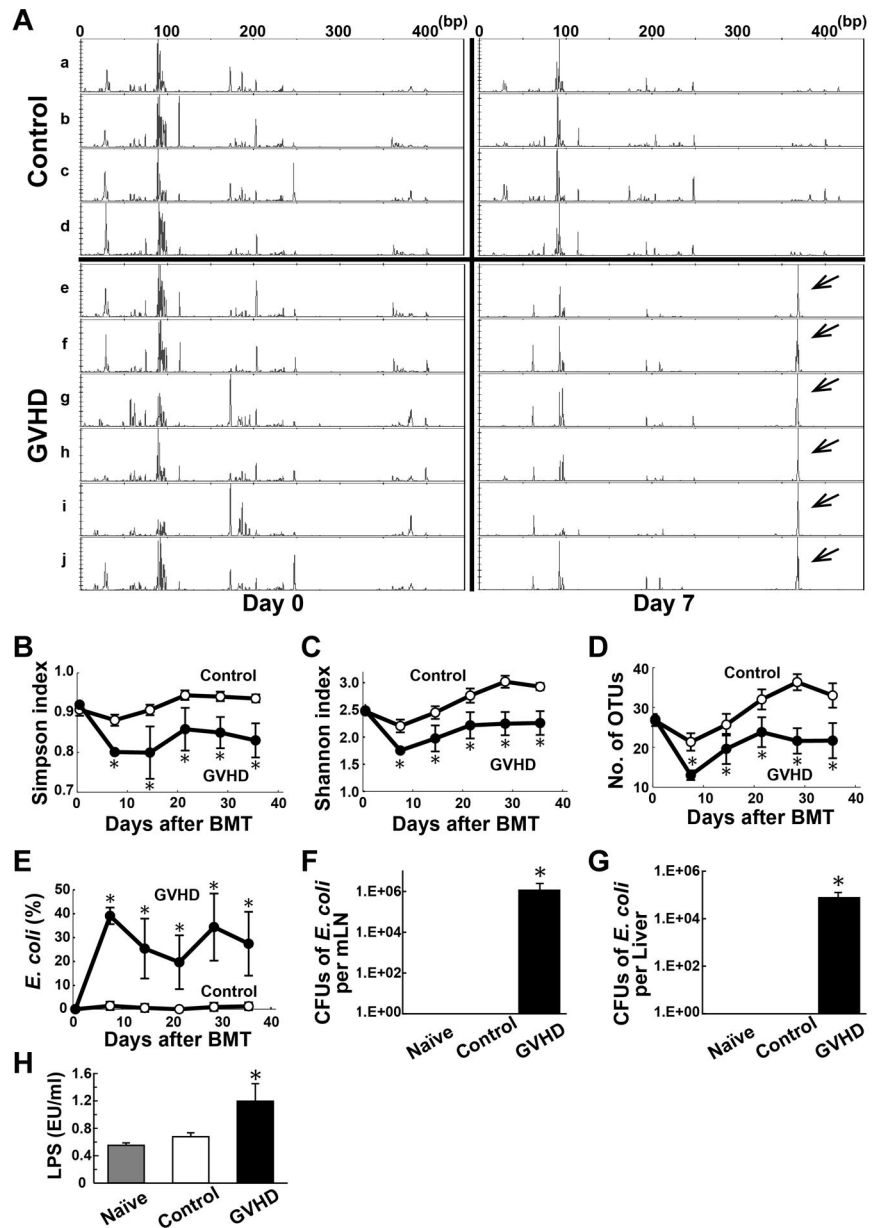
OTUs were slightly decreased with little changes in the RFLP patterns in controls (Figure 3A right top panels); however, in the mice with GVHD, the number of OTUs decreased and the peak heights of OTUs were markedly reduced, with the exception of an aberrantly high peak at 368 bp (Figure 3A right bottom panels). Sequence analysis of subclones from a representative animal from GVHD group showed that proportions of both Firmicutes and Bacteroidetes, which are the major enteric commensals,^{12,15} were decreased in mice with GVHD on day 7 compared with those before BMT (Firmicutes; 22.9% vs 52.1%, Bacteroidetes; 2.1% vs 13.5%, respectively).

These compositional changes in the intestinal microflora were consistently observed in all mice with GVHD. Diversity of the microbial community, which corresponds to the RFLP banding patterns, was significantly reduced in mice with GVHD at all time points, as assessed by the Simpson index of diversity,²⁶ Shannon diversity index,²⁷ and the number of OTUs counted (Figure 3B–D).

Overwhelming outgrowth of *E coli* in mice with GVHD

A single high peak at 368bp was noted in mice with GVHD (Figure 3A arrows). To identify the bacteria included at this OTU, plasmid DNA from the corresponding clone was purified. DNA sequencing showed a high similarity to 16S rRNA from *E coli* with a similarity rate of more than 99.5%. The proportion of *E coli* in the microbiota, which was defined as the ratio of the area of OTU for *E coli* to the total areas of all OTUs, was dramatically higher 7 days after BMT and remained higher in mice with GVHD throughout the entire observation period; however, *E coli* remained to be a small portion of the microbial population in controls (Figure 3E). Next, we evaluated whether the high levels of *E coli* in the intestine could be associated with the development of systemic infection in mice with GVHD. Seven days after BMT, mLNs and livers were harvested. *E coli* was identified from samples taken from mice with GVHD, but not the controls. The number of CFUs of *E coli* was significantly higher in the mLNs and liver of mice with GVHD than those in controls (Figure 3F–G). Serum LPS levels were also significantly higher in mice with GVHD than in controls (Figure 3H).

Figure 3. Perturbation of normal intestinal microbiota in GVHD. Fecal pellets were collected before and after a B6 → B6D2F1 BMT weekly and intestinal microbiota was characterized by RFLP analysis of 16S rRNA gene libraries constructed from each sample of fecal pellets and digested with *HhaI* (n = 6 / group). (A) Representative RFLP patterns are shown in control group (a-d) and GVHD group (e-j). Left panels indicate before BMT; right panels, 7 days after BMT. Arrows indicate an OTU for *Escherichia coli*. (B-D) Time course changes in flora diversity after BMT determined by using Simpson index (B), Shannon index (C), and numbers of OTUs (D). (E) Time course changes in the proportion of *E. coli*. (F-G) Samples of mLNs and liver were harvested on day 7 and CFUs of *E. coli* were enumerated by the culture-based and microbiologic identification method. (H) Serum LPS levels on day 7. Data are representative of 3 similar experiments and are shown as mean ± SE (**P* < .05).



The composition of intestinal microflora in animals can differ depending on the environment and other factors.³² Therefore, we used mice purchased from multiple vendors; however, the resulting patterns of dysbiosis were similar, regardless of the origin source of the mice. In addition, we found similar changes in the intestinal microbiota of another haplotype, the mismatched B6 → B6C3F1 (H-2^{b/k}) model of BMT. Diversity of intestinal flora was lost with an outgrowth of *E. coli* 7 days after BMT and thereafter only in mice with GVHD (data not shown).

Association between changes in intestinal microbiota and GVHD severity

Further studies were conducted to determine whether there could be an association between the magnitude of changes observed in the intestinal flora and GVHD severity. Diversity of the flora, as determined by the Simpson index, Shannon index, and the number of OTUs was inversely correlated with GVHD severity (Figure

4A-C). On the other hand, the proportion of *E. coli* in the intestinal flora was positively correlated with GVHD severity (Figure 4D).

Delayed alteration in intestinal microbial diversity after MHC-matched BMT

To further confirm that our observations were not strain or model dependent, we evaluated whether the observed changes in the intestinal flora could be observed in a clinically relevant, MHC-matched, and minor histocompatibility antigen-mismatched C3H.Sw (H-2^b) → B6 (H-2^b) model of BMT, in which GVHD developed more slowly and was less severe compared with the MHC-mismatched models of GVHD (Figure 5A-B).³³ Again, normal microbial diversity was lost in mice with GVHD and *E. coli* levels were higher at 2 weeks after BMT and thereafter (Figure 5C-F). Thus, changes in the intestinal microbiota occurred more slowly in this model, at least compared with the MHC-mismatched model of GVHD; furthermore, the changes occurred in parallel with the

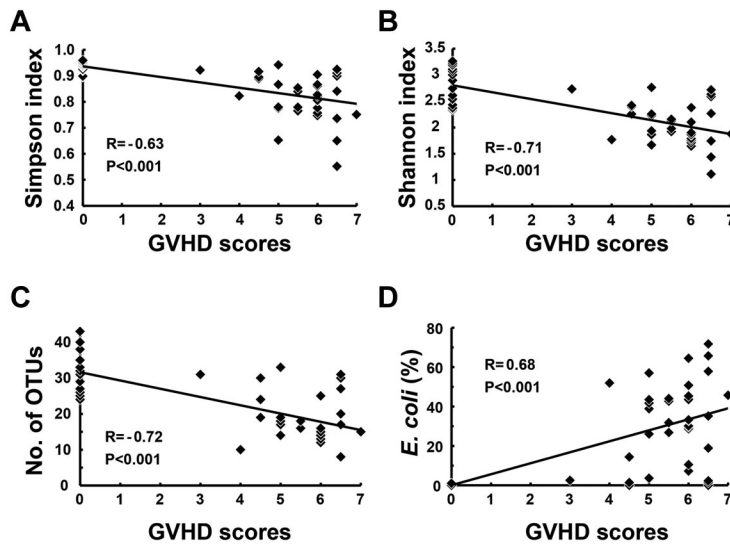


Figure 4. Correlation between the degree of flora changes and GVHD severity. Lethally irradiated B6D2F1 mice were transplanted with TCD BM with T cells from B6 donors ($n = 6$ /group). Fecal pellets were collected at day 0 and weekly thereafter and intestinal microbiota was characterized by RFLP analysis. Clinical GVHD scores and various parameters of the flora diversity and the proportion of *E coli* in the intestinal flora at various time points from each mice were plotted. Correlations of GVHD clinical scores and Simpson index (A), Shannon index (B), numbers of OTUs (C), and proportion of *E coli* (D). The regression line was plotted with all data. Data from 2 independent experiments were combined. R: correlation coefficient.

slower development of GVHD. It should be noted that normal flora diversity was recovered and *E coli* returned to a normally small population among the intestinal microbiota late after BMT, as GVHD severity reduced. No mortality was observed in allogeneic animals after regaining normal intestinal flora.

Loss of Paneth cells and the dysbiosis by a mechanism independent on conditioning

We addressed whether GVHD mediates Paneth cell injury and the alteration of the composition of the intestinal flora by a mechanism dependent on radiation-induced intestinal tract damage in the B6 \rightarrow B6D2F1 BMT model without conditioning, as previously described.⁷ Unirradiated B6D2F1 mice were intravenously injected with 12×10^7 splenocytes from syngeneic or allogeneic B6 donors on day 0. In this model, GVHD occurred early after BMT at a peak around day 20 but was spontaneously improved (Figure 6A-C). Numbers of Paneth cells were markedly reduced 2 weeks after BMT but gradually returned to normal levels thereafter in allogeneic animals (Figure 6D). The changes in the intestinal microbiota occurred in parallel with the degree of GVHD severity and Paneth cell injury; normal microbial diversity was lost with the outgrowth of *E coli*, but was gradually restored later after BMT in allogeneic animals (Figure 6E-H).

Oral administration of antibiotics inhibited the outgrowth of *E coli* and ameliorated GVHD

Finally, we evaluated whether modifying the enteric flora using oral antibiotics could ameliorate GVHD. Lethally irradiated B6D2F1 mice were transplanted with 5×10^6 TCD BM cells with or without 2×10^6 T cells from B6-Ly5.1 (CD45.1⁺) donors. Polymyxin B (PMB), an antibiotic primarily effective against gram-negative bacteria, was administered by daily oral gavage at a dose of 100 mg/kg from day -4 until day 28 after BMT. Analysis of fecal pellets 7 days after BMT showed that the outgrowth of *E coli* was inhibited in mice treated with PMB compared with those treated with diluent (Figure 7A). PMB suppressed the outgrowth of *E coli* during PMB treatment; however, *E coli* levels increased after cessation of PMB treatment (Figure 7B). Notably, administration of PMB significantly reduced mortality and morbidity of GVHD (Figure 7C-D). Donor (CD45.1⁺) T-cell expansion (Figure 7E) and pathology scores of the small intestine (Figure 7F) were significantly reduced in PMB-treated mice compared with those in controls.

Discussion

Intestinal GVHD is critical for determining the outcome of allogeneic BMT. Paneth cells are essential regulators of the

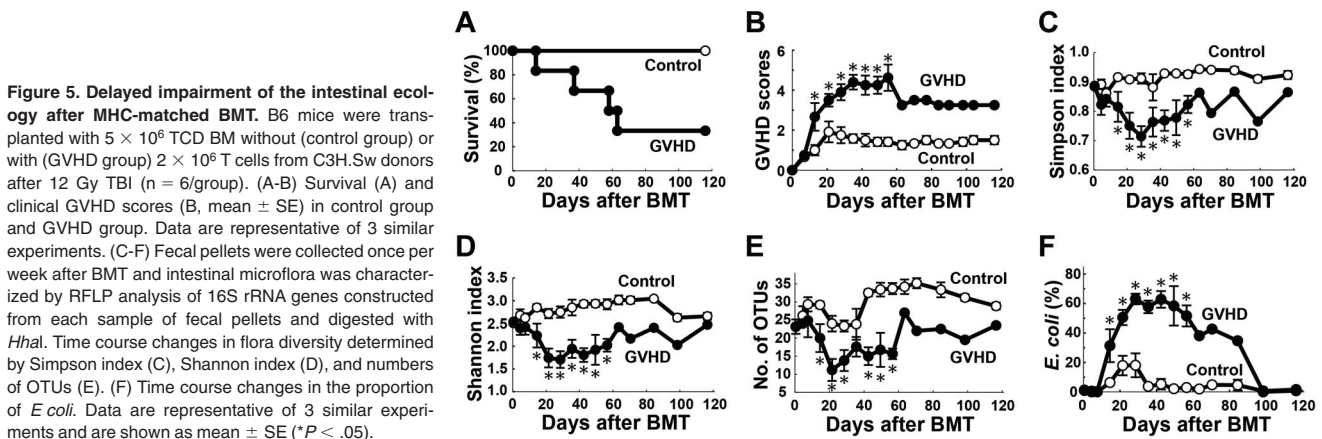
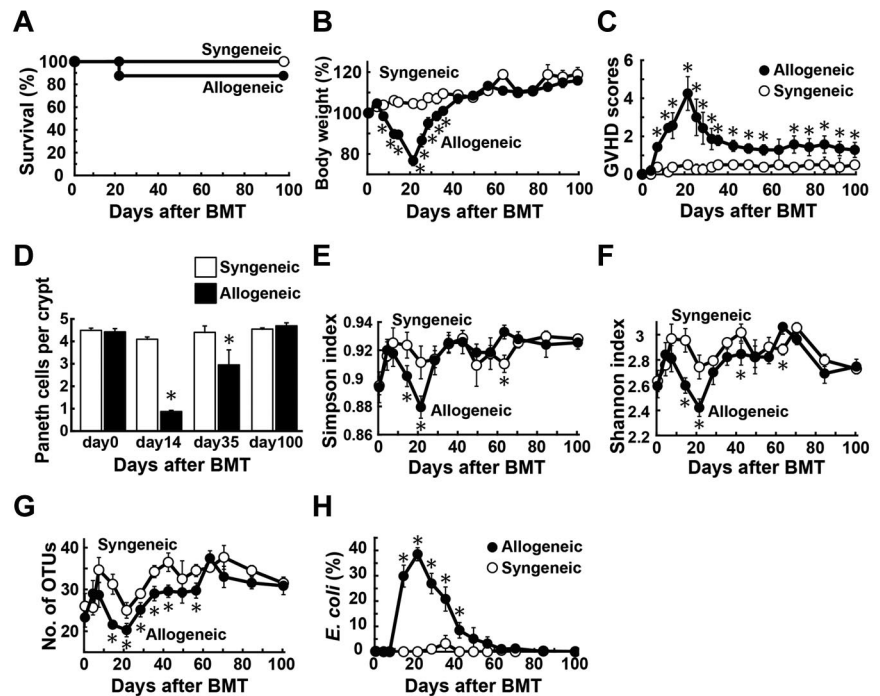


Figure 5. Delayed impairment of the intestinal ecology after MHC-matched BMT. B6 mice were transplanted with 5×10^6 TCD BM without (control group) or with (GVHD group) 2×10^6 T cells from C3H.Sw donors after 12 Gy TBI ($n = 6$ /group). (A-B) Survival (A) and clinical GVHD scores (B, mean \pm SE) in control group and GVHD group. Data are representative of 3 similar experiments. (C-F) Fecal pellets were collected once per week after BMT and intestinal microflora was characterized by RFLP analysis of 16S rRNA genes constructed from each sample of fecal pellets and digested with *HhaI*. Time course changes in flora diversity determined by Simpson index (C), Shannon index (D), and numbers of OTUs (E). (F) Time course changes in the proportion of *E coli*. Data are representative of 3 similar experiments and are shown as mean \pm SE (* $P < .05$).

Figure 6. Paneth cell injury and the dysbiosis developed by a mechanism independent on conditioning. Unirradiated B6D2F1 mice were transplanted with 12×10^7 splenocytes from syngeneic or allogeneic MHC-mismatched B6 donors on day 0 ($n = 6/\text{group}$). Survival (A), changes in body weight (B, mean \pm SE), clinical GVHD scores (C, mean \pm SE), and (D) quantification of Paneth cells per crypt in the small intestine were shown. (E-H) Fecal pellets were collected before and after BMT weekly and intestinal microbiota was characterized by RFLP analysis of 16S rRNA gene libraries constructed from each sample of fecal pellets and digested with *HhaI*. Time course changes in flora diversity determined by using Simpson index (E), Shannon index (F), numbers of OTUs (G), and the proportion of *E coli* (H). Data from 2 independent experiments were combined and are shown as mean \pm SE.



composition of commensal microbiota in the intestine, and they maintain the intestinal microbial environment by secreting various microbial peptides. In this study, we found that damage to Paneth cells by GVHD results in dramatically reduced expression of α -defensins in the small intestines and perturbed normal intestinal environment. These changes occurred in the absence of conditioning irradiation, thus indicating a mechanism dependent on allogeneic T-cell responses. However, Paneth cell loss occurred earlier and more prolonged in mice receiving irradiation than in unirradiated mice, suggesting that conditioning enhanced Paneth cell damage directly and indirectly by accelerating GVHD. The diversity of the intestinal microflora was lost with overwhelming expansion of specific bacteria, such as *E coli*, which are normally a very small proportion of the intestinal microbial communities. Paneth cells secrete α -defensins into the intestinal lumen within minutes after sensing gram-negative and gram-positive bacteria and their components, such as LPS, through activation of pattern recognition receptors.^{23,34} α -defensins are the most potent antimicrobial peptides and account for 70% of the bactericidal peptide activity released from Paneth cells.^{11,23} α -Defensins are released in the small bowel lumen and persist as intact and functional forms throughout the intestinal tract.³⁵ Thus, they shape the composition of the microbiota in the entire intestine. Importantly, α -defensins have selective bactericidal activity against noncommensals, such as *Salmonella enterica*, *E coli*, *Klebsiella pneumoniae*, and *Staphylococcus aureus*, although exhibiting minimal bactericidal activity against commensals.^{28,29} Such bacteria-dependent bactericidal activities of α -defensins are in tune with intestinal environment and may explain why the absence of α -defensins causes the alterations in the intestinal microbiota in GVHD. Because commensals have a profound influence on nutritional, physiologic, and metabolic function of the host,^{14,36,37} reduction of commensals may have ill effects on the host with GVHD. In this study, *E coli* was the dominant enteric microbe in mice with GVHD among multiple strains of mice. However, the dominant species may differ between studies because of the differences in several factors, including differences in the maintenance protocols used to feed and care for the experimental animals.³² Nonetheless, our study confirms and

further extends a recent study showing the intestinal flora change, with an increase in gram-negative *Enterobacteriaceae* family members including *E coli*, after allogeneic BMT in mice.¹⁸

Alteration of the intestinal microbiota has been shown in experimental and clinical inflammatory bowel diseases, allergies, diabetes, and obesity.^{13,38-42} This study provides several lines of evidence that suggest a close association between dysbiosis and GVHD. Mice without GVHD maintained normal microbiota after BMT, and dysbiosis only occurred in mice with GVHD, independent of the murine models used. The normal intestinal environment was never restored as long as severe GVHD persisted, but was restored when tolerance was induced after transplant. In mice with GVHD, the degree of changes to the microflora was significantly correlated to GVHD severity and MHC disparity between the donor and recipient. Furthermore, modifying enteric flora by oral administration of antibiotics inhibited the outgrowth if *E coli* and ameliorated GVHD. The flora shift toward the widespread prevalence of gram-negative bacteria increases the translocation of LPS, the major component of the outer membrane of gram-negative bacteria, into systemic circulation and further accelerates GVHD by stimulates production of inflammatory cytokines, such as TNF- α and IL-1, which are critical effector molecules that mediate GVHD.^{22,43-45} Thus, GVHD and the dysbiosis can lead to a positive feedback loop that increases the translocation of LPS, thereby resulting in further cytokine production, progressive intestinal injury, and systemic GVHD acceleration. Earlier seminal studies in the 1960s-1970s suggested that GVHD is reduced in germfree mice or by treatment with poorly absorbable antibiotics.³⁻⁶ A recent study also demonstrated that modifying the enteric flora using a probiotic microorganism reduced GVHD in mice.⁴⁶ Thus, our study again highlights an important role of oral antibiotics administration on GVHD. Our study demonstrated that dominant bacteria in the intestinal microbiota cause systemic infection. There was a microbiologic evidence of infection in mice with severe GVHD and a correlation between severity of infection and GVHD, thus suggesting that severe bacteremia, probably caused by the translocation of enteric bacteria, can also contribute to GVHD mortality, as previously suggested.^{6,46} Indeed, septicemia by gram-negative rods

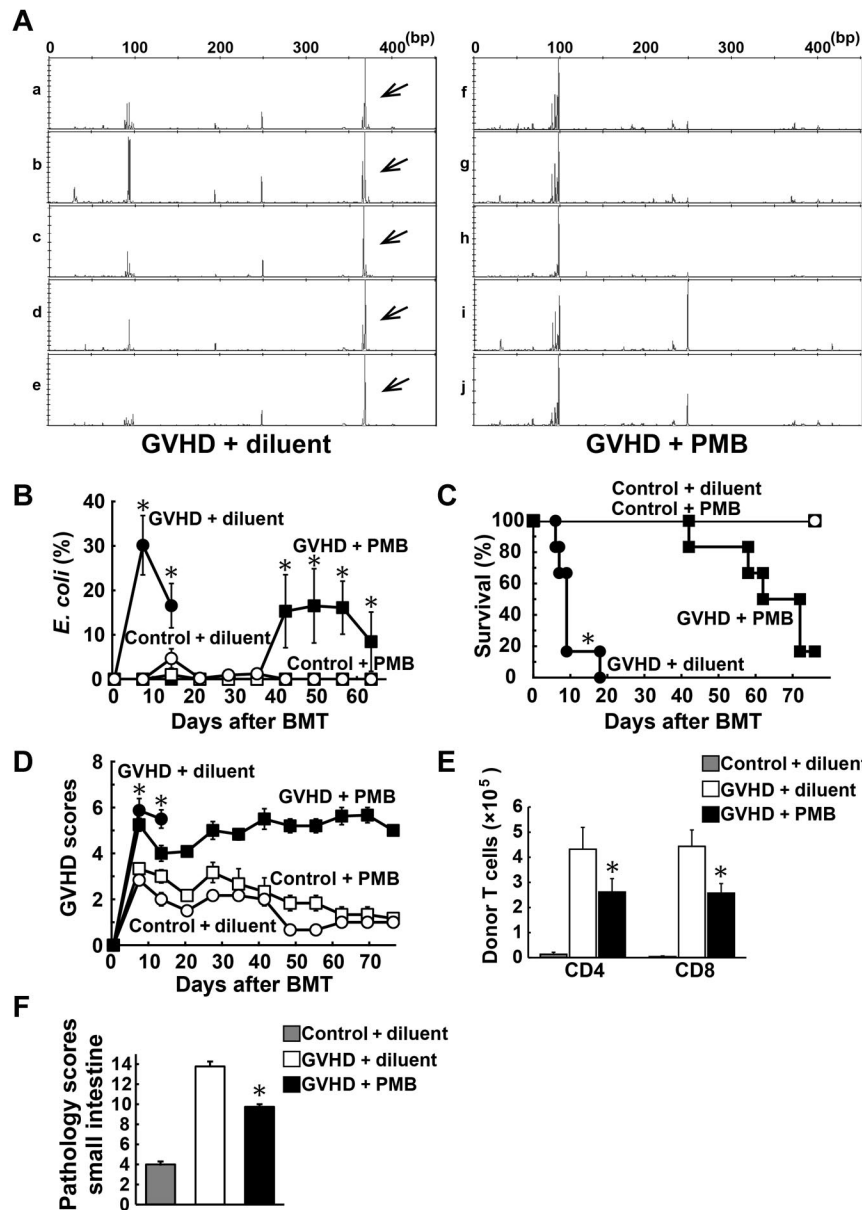


Figure 7. Oral administration of polymyxin B ameliorated GVHD. Lethally irradiated B6D2F1 mice were transplanted with 5×10^6 TCD BM without or with 2×10^6 T cells from B6 or B6-Ly5.1 (CD45.1⁺) donors. Polymyxin B (PMB; 100 mg/kg) or diluent was administered by daily oral gavage from day -4 until day 28 after BMT. (A) Fecal pellets were collected once per week after BMT and intestinal microflora was characterized by RFLP analysis of 16S rRNA genes constructed from each sample of fecal pellets and digested with *HhaI*. Representative RFLP patterns are shown in mice with GVHD receiving diluent (a-e) and those with PMB (f-j) 7 days after BMT. Arrows indicate an OTU for *E. coli*. (B) Time course changes in the proportion of *E. coli* ($n = 6-12$ /group). Survival (C) and clinical GVHD scores (D, mean \pm SE) after BMT are shown ($n = 6-12$ /group). Data from 2 independent experiments were combined. (E) Numbers of donor (CD45.1⁺) T cells in mLNs on day 5 ($n = 20$ /group). (F) Pathology scores of the small intestine on day 7 ($n = 20$ /group). Data from 3 independent experiments were combined and are shown as mean \pm SE (* $P < .05$).

is one of the most frequent causes of death in patients with severe intestinal GVHD.

There are other interfaces that exist between the environment and the host, such as the skin and airways. Epithelial cells in these tissues can also release antimicrobial peptides such as β -defensins in response to bacteria and LPS.⁴⁷ GVHD-mediated epithelial cell damage of these tissues may also impair the local secretion of antimicrobial peptides, leading to aberrant overgrowth of pathogens and development of dermal infections or pneumonia, which are frequently observed in patients with GVHD. Furthermore, the development of these pathologic conditions may be associated with the unique tissue specificity of GVHD for tissues that are in contact with high microbial loads, such as the skin, liver, intestine, and lung.

Intestinal epithelial cells are continuously regenerated from ISCs, which are required to regenerate damaged sections of the intestinal epithelium.⁴⁸ Paneth cells are derived from ISCs and serve as a niche for ISCs.⁸ Our previous⁷ and current studies addressed intestinal GVHD at the cellular level, and demonstrated that ISCs and their niche Paneth cells could survive pretransplant

conditioning and regenerate injured epithelium by conditioning in the absence of GVHD. However, both ISCs and Paneth cells are targeted by GVHD, resulting in an impairment of the physiologic repair mechanisms of injured epithelium, although it remains to be elucidated whether Paneth cell loss is induced by direct cytotoxicity to Paneth cell itself or secondary to the loss of ISCs. This phenomenon may explain the prolonged and refractory nature of clinical intestinal GVHD. These new insights will help to establish new therapeutic strategies that can be used to prevent and treat GVHD and related infections and improve the clinical outcome of allogeneic BMT.

Acknowledgments

This study was supported by grants from Japan Society for the Promotion of Science (JSJP) KAKENHI (23659490 to T.T., 23390193 to T.A., and 22592029 to K.N.), Health and Labor Science Research Grants (T.T.), the Foundation for Promotion of Cancer Research (Tokyo, Japan; to T.T.), the Knowledge Cluster, Sapporo Bio-S from Ministry of

Education, Culture, Sports, Science and Technology (MEXT; Tokyo, Japan; to T.A.), Yakult Bio-Science Foundation (Tokyo, Japan; to Y.E.), and SENSHIN Medical Research Foundation (to T.T.).

data, and wrote the paper; S.T., H.O., S. Shimoji, K.N., H.U., S. Shimoda, and H.I. conducted experiments; and N.S., T.A., and K.A. supervised experiments.

Conflict-of-interest disclosure: The authors declare no competing financial interests.

Correspondence: Takanori Teshima, Center for Cellular and Molecular Medicine, Kyushu University Hospital, 3-1-1 Maidashi, Higashi-ku, Fukuoka 812-8582, Japan; e-mail: tteshima@cancer.med.kyushu-u.ac.jp.

Authorship

Contribution: Y.E. and T.T. developed the conceptual framework of the study, designed the experiments, conducted studies, analyzed

References

- Bossaer JB, Hall PD, Garrett-Mayer E. Incidence of vancomycin-resistant enterococci (VRE) infection in high-risk febrile neutropenic patients colonized with VRE. *Support Care Cancer*. 2010; 19(2):231-237.
- Winston DJ, Gale RP, Meyer DV, Young LS. Infectious complications of human bone marrow transplantation. *Medicine*. 1979;58(1):1-31.
- van Bekkum D, Vos O. Treatment of secondary disease in radiation chimeras. *Int J Radiat Biol*. 1961;3:173-181.
- Jones JM, Wilson R, Bealmeas PM. Mortality and gross pathology of secondary disease in germ-free mouse radiation chimeras. *Radiation Res*. 1971;45(3):577-588.
- van Bekkum DW, Roodenburg J, Heidt PJ, van der Waaij D. Mitigation of secondary disease of allogeneic mouse radiation chimeras by modification of the intestinal microflora. *J Nat Cancer Inst*. 1974;52(2):401-404.
- Heit H, Heit W, Kohne E, Fliedner TM, Hughes P. Allogeneic bone marrow transplantation in conventional mice: I. Effect of antibiotic therapy on long term survival of allogeneic chimeras. *Blut*. 1977;35(2):143-153.
- Takashima S, Kadowaki M, Aoyama K, et al. The Wnt agonist R-spondin1 regulates systemic graft-versus-host disease by protecting intestinal stem cells. *J Exp Med*. 2011;208(2):285-294.
- Sato T, van Es JH, Snippert HJ, et al. Paneth cells constitute the niche for Lgr5 stem cells in intestinal crypts. *Nature*. 2011;469(7330):415-418.
- Selsted ME, Harwig SS. Determination of the disulfide array in the human defensin HNP-2. A covalently cyclized peptide. *J Biol Chem*. 1989; 264(7):4003-4007.
- Ganz T, Selsted ME, Lehrer RI. Defensins. *Eur J Haematol*. 1990;44(1):1-8.
- Salzman NH, Hung K, Haribhai D, et al. Enteric defensins are essential regulators of intestinal microbial ecology. *Nat Immunol*. 2010;11(1):76-83.
- Eckburg PB, Bik EM, Bernstein CN, et al. Diversity of the human intestinal microbial flora. *Science*. 2005;308(5728):1635-1638.
- Qin J, Li R, Raes J, et al. A human gut microbial gene catalogue established by metagenomic sequencing. *Nature*. 2010;464(7285):59-65.
- Hill DA, Artis D. Intestinal bacteria and the regulation of immune cell homeostasis. *Ann Rev Immunol*. 2010;28:623-667.
- Zoetendal EG, Akkermans AD, De Vos WM. Temperature gradient gel electrophoresis analysis of 16S rRNA from human fecal samples reveals stable and host-specific communities of active bacteria. *Appl Environ Microbiol*. 1998;64(10): 3854-3859.
- Kurokawa K, Itoh T, Kuwahara T, et al. Comparative metagenomics revealed commonly enriched gene sets in human gut microbiomes. *DNA Res*. 2007;14(4):169-181.
- Hooper LV, Macpherson AJ. Immune adaptations that maintain homeostasis with the intestinal microbiota. *Nature Rev Immunol*. 2010;10(3):159-169.
- Heimesaat MM, Nogai A, Bereswill S, et al. MyD88/TLR9 mediated immunopathology and gut microbiota dynamics in a novel murine model of intestinal graft-versus-host disease. *Gut*. 2010; 59(8):1079-1087.
- Ubeda C, Taur Y, Jenq RR, et al. Vancomycin-resistant Enterococcus domination of intestinal microbiota is enabled by antibiotic treatment in mice and precedes bloodstream invasion in humans. *J Clin Invest*. 2010;120(12):4332-4341.
- Cooke KR, Kobzik L, Martin TR, et al. An experimental model of idiopathic pneumonia syndrome after bone marrow transplantation. I. The roles of minor H antigens and endotoxin. *Blood*. 1996;88: 3230-3239.
- Asakura S, Hashimoto D, Takashima S, et al. Allogeneic expression on non-hematopoietic cells reduces graft-versus-leukemia effects in mice. *J Clin Invest*. 2010;120(7):2370-2378.
- Teshima T, Ordemann R, Reddy P, et al. Acute graft-versus-host disease does not require allogeneic expression on host epithelium. *Nat Med*. 2002;8(6):575-581.
- Ayabe T, Satchell DP, Wilson CL, Parks WC, Selsted ME, Ouellette AJ. Secretion of microbicidal alpha-defensins by intestinal Paneth cells in response to bacteria. *Nat Immunol*. 2000;1(2): 113-118.
- Li F, Hullar MA, Lampe JW. Optimization of terminal restriction fragment polymorphism (TRFLP) analysis of human gut microbiota. *J Microbiol Methods*. 2007;68(2):303-311.
- Hayashi H, Takahashi R, Nishi T, Sakamoto M, Benno Y. Molecular analysis of jejunal, ileal, caecal and recto-sigmoidal human colonic microbiota using 16S rRNA gene libraries and terminal restriction fragment length polymorphism. *J Med Microbiol*. 2005;54(Pt 11):1093-1101.
- Simpson EH. Measurement of diversity. *Nature*. 1949;163:688.
- Shannon C. A mathematical theory of communication. *Bell System Technol J*. 1948;27:379-423.
- Ouellette AJ, Hsieh MM, Nosek MT, et al. Mouse Paneth cell defensins: primary structures and antibacterial activities of numerous cryptdin isoforms. *Infect Immun*. 1994;62(11):5040-5047.
- Masuda K, Sakai N, Nakamura K, Yoshioka S, Ayabe T. Bactericidal activity of mouse alpha-defensin cryptdin-4 predominantly affects non-commensal bacteria. *J Innate Immun*. 2011;3(3): 315-326.
- Liu WT, Marsh TL, Cheng H, Forney LJ. Characterization of microbial diversity by determining terminal restriction fragment length polymorphisms of genes encoding 16S rRNA. *Appl Environ Microbiol*. 1997;63(11):4516-4522.
- Hayashi H, Sakamoto M, Benno Y. Phylogenetic analysis of the human gut microbiota using 16S rDNA clone libraries and strictly anaerobic culture-based methods. *Microbiol Immunol*. 2002; 46(8):535-548.
- Ivanov II, Atarashi K, Manel N, et al. Induction of intestinal Th17 cells by segmented filamentous bacteria. *Cell*. 2009;139(3):485-498.
- Shlomchik WD, Couzens MS, Tang CB, et al. Prevention of graft versus host disease by inactivation of host antigen-presenting cells. *Science*. 1999;285(5426):412-415.
- Vaishnava S, Behrendt CL, Ismail AS, Eckmann L, Hooper LV. Paneth cells directly sense gut commensals and maintain homeostasis at the intestinal host-microbial interface. *Proc Natl Acad Sci U S A*. 2008; 105(52):20858-20863.
- Mastroianni JR, Ouellette AJ. Alpha-defensins in enteric innate immunity: functional Paneth cell alpha-defensins in mouse colonic lumen. *J Biol Chem*. 2009;284(41):27848-27856.
- Hooper LV, Midtvedt T, Gordon JL. How host-microbial interactions shape the nutrient environment of the mammalian intestine. *Annu Rev Nutr*. 2002;22:283-307.
- Bäckhed F, Ley RE, Sonnenburg JL, Peterson DA, Gordon JL. Host-bacterial mutualism in the human intestine. *Science*. 2005;307(5717):1915-1920.
- Ley RE, Turnbaugh PJ, Klein S, Gordon JL. Microbial ecology: human gut microbes associated with obesity. *Nature*. 2006;444(7122):1022-1023.
- Turnbaugh PJ, Ley RE, Mahowald MA, Magrini V, Mardis ER, Gordon JL. An obesity-associated gut microbiome with increased capacity for energy harvest. *Nature*. 2006;444(7122):1027-1031.
- Manichanh C, Rigottier-Gois L, Bonnaud E, et al. Reduced diversity of faecal microbiota in Crohn's disease revealed by a metagenomic approach. *Gut*. 2006;55(2):205-211.
- Bollyky PL, Bice JB, Sweet IR, et al. The toll-like receptor signaling molecule Myd88 contributes to pancreatic beta-cell homeostasis in response to injury. *PLoS One*. 2009;4(4):e5063.
- Penders J, Thijs C, van den Brandt PA, et al. Gut microbiota composition and development of atopic manifestations in infancy: the KOALA Birth Cohort Study. *Gut*. 2007;56(5):661-667.
- Hill GR, Ferrara JL. The primacy of the gastrointestinal tract as a target organ of acute graft-versus-host disease: rationale for the use of cytokine shields in allogeneic bone marrow transplantation. *Blood*. 2000;95(9):2754-2759.
- Nestel FP, Price KS, Seemayer TA, Lapp WS. Macrophage priming and lipopolysaccharide-triggered release of tumor necrosis factor alpha during graft-versus-host disease. *J Exp Med*. 1992;175:405-413.
- Cooke KR, Gerbitz A, Crawford JM, et al. LPS antagonism reduces graft-versus-host disease and preserves graft-versus-leukemia activity after experimental bone marrow transplantation. *J Clin Invest*. 2001;107(12):1581-1589.
- Gerbitz A, Schultz M, Wilke A, et al. Probiotic effects on experimental graft-versus-host disease: let them eat yogurt. *Blood*. 2004;103(11):4365-4367.
- Bals R, Wang X, Meegalla HJ, et al. Mouse beta-defensin 3 is an inducible antimicrobial peptide expressed in the epithelia of multiple organs. *Infect Immun*. 1999;67(7):3542-3547.
- Sato T, Vries RG, Snippert HJ, et al. Single Lgr5 stem cells build crypt-villus structures in vitro without a mesenchymal niche. *Nature*. 2009; 459(7244):262-265.